

Radio pulsars with expected gamma radiation and gamma-ray pulsars as pulsating radio emitters

Igor Fedorovich Malov and Maria Andreevna Timirkееva

Pushchino Radio Astronomy Observatory, Astro Space Center, P. N. Lebedev Physical Institute, Pushchino 142290, Russia; malov@prao.ru

Received 2017 November 7; accepted 2017 December 14

Abstract Pulsars play a crucial astrophysical role as highly energetic compact radio, X-ray and gamma-ray sources. Our previous works show that radio pulsars identified as pulsing gamma-ray sources by the Large Area Telescope (LAT) on board the *Fermi Gamma-Ray Space Telescope* have high values of magnetic field near the light cylinder, two-three orders of magnitude stronger compared with the magnetic fields of radio pulsars: $\log B_{lc}$ (G) are 3.60–3.95 and 1.75 correspondingly. Moreover, their losses of rotational energy are also three orders higher than the corresponding values for the main group of radio pulsars on average: $\log \dot{E}$ (erg s^{-1}) = 35.37–35.53 and 32.64. The correlation between gamma-ray luminosities and radio luminosities is found. It allows us to select those objects from all sets of known radio pulsars that can be detected as gamma-ray pulsars with high probability. We provide a list of such radio pulsars and propose to search for gamma emission from these objects. On the other hand, the known catalog of gamma-ray pulsars contains some sources which are not currently identified as radio pulsars. Some of them have large values of gamma-ray luminosities and according to the obtained correlation, we can expect marked radio emission from these objects. We give the list of such pulsars and expected flux densities to search for radiation at frequencies 1400 and 111 MHz.

Key words: pulsars: individual — gamma-ray bursts: individual — stars: magnetic field

1 INTRODUCTION

The *Fermi* space telescope with the Large Area Telescope (LAT) has detected over 150 new gamma-ray pulsars, which are included in the Second Fermi LAT catalog (hereafter 2FGL catalog, Abdo et al. 2013), increasing their previous number (see, for example, Thompson, 1996) by a factor of several dozen. The analysis of their properties is very important for understanding the nature of pulsed emission. All data on gamma pulsars in our paper were taken from this 2FGL catalog. We have used parameters of known radio pulsars from the ATNF catalog (Manchester et al. 2005).

We have shown earlier (Malov & Timirkееva 2014, Malov & Timirkееva (2015)) that radio pulsars detected as pulsed gamma sources by *Fermi*/LAT are characterized by high magnetic fields at the light cylinder B_{lc} ,

two-three orders of magnitude higher than in gamma quiet radio pulsars (Fig. 1). The mean values of $\log B_{lc}$ (G) are 3.60–3.95 and 1.75, correspondingly. Gamma pulsars also have large values for losses of rotational energy \dot{E} , three orders of magnitude higher than the main bulk of radio pulsars (Fig. 2) with mean values of $\log \dot{E}$ (erg s^{-1}) = 35.37 – 35.53 and 32.64, correspondingly. However, some gamma quiet radio pulsars have values of B_{lc} and \dot{E} two-three orders of magnitude higher than the average over the whole sample. According to our results, we can expect marked gamma emission from such objects. On the other hand, there are gamma-ray pulsars in the 2FGL catalog, which have not been detected as radio pulsars up to now, although their parameters imply that their radio emission must have been registered. The main aim of our paper is to compile a list of gamma ray pulsars with expected radio emission.

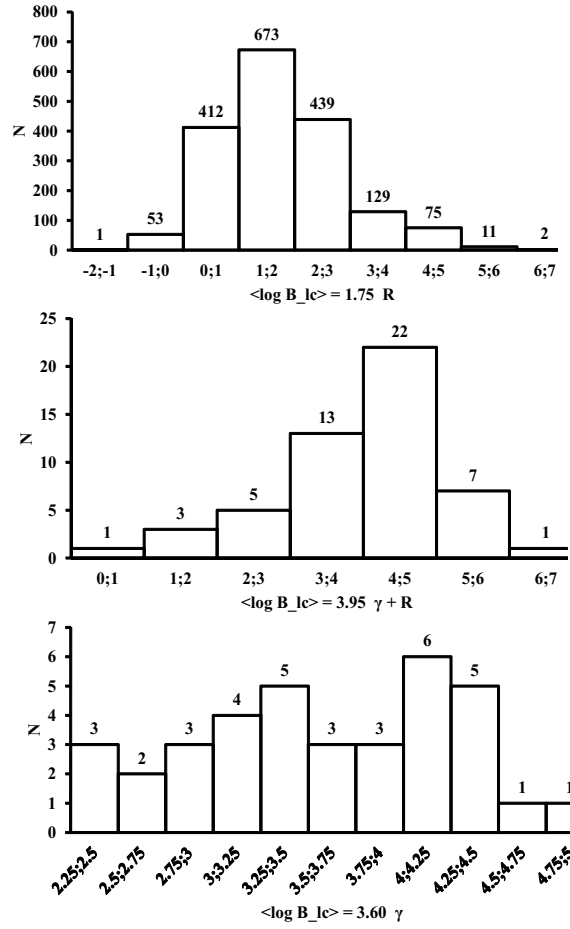


Fig. 1 Distributions of magnetic fields at the light cylinder for gamma quiet radio pulsars (R), gamma-ray pulsars with radio pulsations ($\gamma + R$) and radio quiet gamma-ray pulsars (γ).

2 SAMPLE OF PULSARS USED IN THIS STUDY

We have applied two criteria: magnetic fields at the light cylinder $B_{lc} > 10^3$ G and losses of rotational energy $\dot{E} > 3 \times 10^{34}$ erg s $^{-1}$. It is worth noting that both of these parameters are determined as functions of the pulsar period and its derivative

$$\dot{E} = \frac{4\pi^2 I \dot{P}}{P^3}, \quad (1)$$

$$B_{lc} = B_s \left(\frac{R_*}{r_{lc}} \right)^3 = \frac{8\pi^3 B_s R_*^3}{c^3 P^3} = \frac{8\pi^3 A R_*^3 \dot{P}^{1/2}}{c^3 P^{5/2}}. \quad (2)$$

The last expression has been derived by considering the dipole structure of magnetic fields through the whole pulsar magnetosphere. Moreover, it is suggested that the pulsar braking is caused by magneto-dipole radiation. Here $I \sim 10^{45}$ g cm 2 is the moment of inertia, $R_* \sim 10^6$ cm is

the radius of the neutron star and c is the speed of light,

$$A = \left(\frac{3Ic^3}{2\pi^2 R_*^6} \right)^{1/2}. \quad (3)$$

This means that there is an evident relation between \dot{E} and B_{lc} . However, it is reasonable to take both of these parameters into account, since their physical meanings differ. The losses of rotational energy characterize the main source of pulsar energy for all processes in its magnetosphere, but the quantity B_{lc} determines the emission mechanism near the light cylinder.

We exclude pulsars in globular clusters and binary systems from the analysis, since their observed characteristics can be distorted by the influence of other nearby stars, and also J1836+5925, J2021+3651, J2021+4026 and J2030+3641 which have estimated efficiency for transforming rotational energy into gamma emission, $\eta = L_\gamma / \dot{E}$, larger than 100%. Such high values of η can be caused by considering their radiation to be isotropic. However, the known models of gamma emission (see,

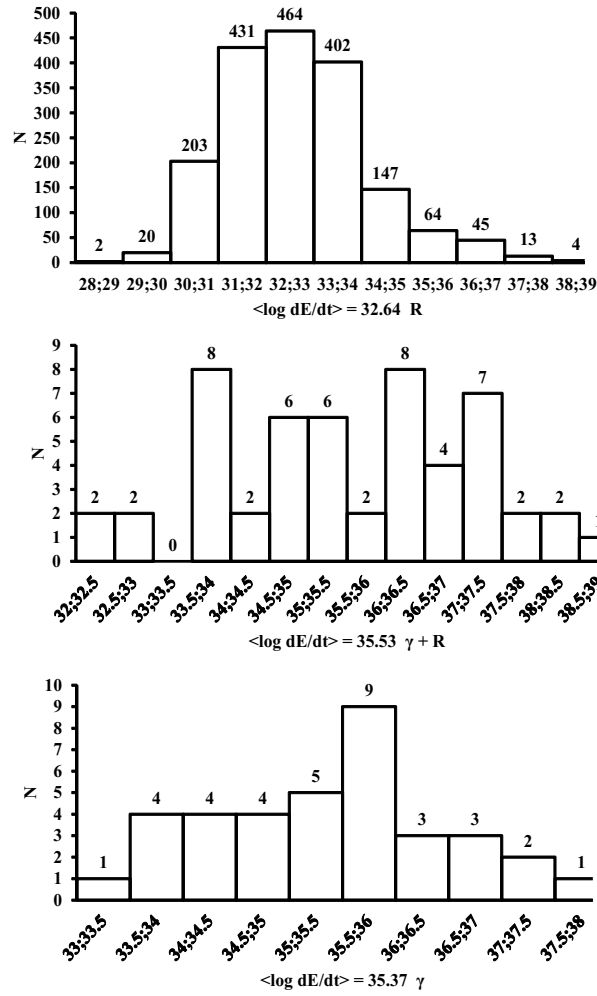


Fig. 2 Distributions of rotational energy losses for three samples of pulsars, as in Fig. 1.

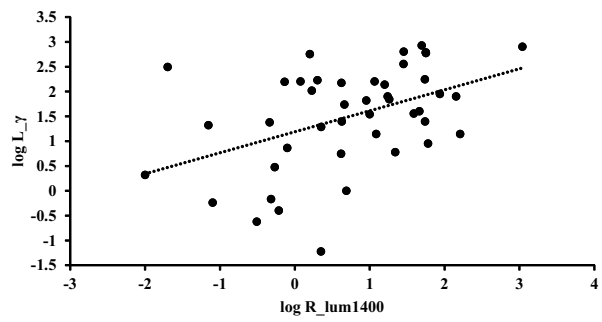


Fig. 3 The relationship between radio and gamma-ray luminosities (see text).

for example, Pierbattista et al. 2012) indicate that such emission is restricted to a rather narrow beam and the real luminosity must be lower than what is given in Abdo et al. (2013). The analyzed sample is presented in Table 1. It contains values of pulsar periods P (s), rota-

tional energy losses \dot{E} (erg s^{-1}), magnetic fields B_{lc} (G) at the light cylinders, radio luminosities $R_{lum1400}$ ($\text{mJy} \times \text{kpc}^2$) and gamma-ray luminosities L_{γ} (erg s^{-1})/ 10^{33} . Comparing radio luminosities $R_{lum1400}$ from the ATNF Pulsar Catalogue and gamma-ray luminosities from the

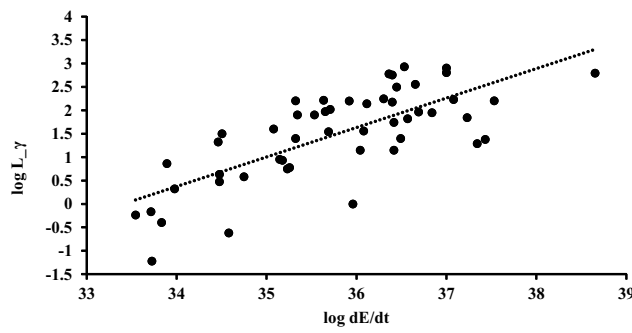


Fig. 4 Dependence of gamma-ray luminosity on losses of rotational energy.

2FGL catalog for 44 pulsars (see Table 1), we obtain the following relationship (Fig. 3)

$$\log L_\gamma = (0.42 \pm 0.12) \log R_{\text{lum}1400} + 1.19 \pm 0.17, \quad (4)$$

with a correlation coefficient $K = 0.45$ and probability of arising from a random distribution $p = 2.5 \times 10^{-3}$. Gamma-ray luminosities in relationship (4) and in Figure 3 are given as $L_\gamma = L(\text{erg s}^{-1})/10^{33}$. To obtain Equation (4), we have used data for all known gamma-ray pulsars. This equation can be applied to predict probable gamma-ray emission from known radio pulsars.

It is worth noting that relationship (4) is a consequence of the dependence of pulsar luminosities, in all ranges, on the losses of their rotational energies \dot{E} . As an illustration of this conclusion, Figure 4 shows the dependence $L_\gamma(\dot{E})$ using data from Manchester et al. (2005) and Abdo et al. (2013).

The equation describing the line in Figure 4 has the following form

$$\log L_\gamma(\text{erg s}^{-1}) = (0.63 \pm 0.08) \log \dot{E}(\text{erg s}^{-1}) - 21.05 \pm 2.93, \quad (5)$$

for which the correlation coefficient is $K = 0.74$ and the probability of arising from a random distribution is $p < 10^{-3}$.

The correlation between \dot{E} and L_γ was obtained earlier by many authors for different samples of pulsars (see, for example, Loginov & Malov 2014).

3 POTENTIAL GAMMA-RAY PULSARS

Using Equation (4) for pulsars with $\dot{E} > 3 \times 10^{34} \text{ erg s}^{-1}$ and $B_{\text{lc}} > 10^3 \text{ G}$, we give estimates of the expected gamma-ray luminosities with uncertainties in the last column.

These 107 pulsars (see Table 2) can be detected in the gamma-ray range with rather high probability. Some assurance comes from recent detections of gamma emission from several studied objects in Table 2 after publication of the Second Fermi LAT pulsar catalog (with references denoted by superscripts a , b and c in Table 2). The estimates made by these authors are indicated in parentheses. Their real physical estimates are numerically close to our predicted values for most objects. These objects are not in 2FGL. However, some of them were discovered after publication of 2FGL, and we are sure that other sources from Table 2 can be registered in future observations.

4 GAMMA-RAY PULSARS WITH EXPECTED RADIO RADIATION

Table 1 contains some pulsars with certain gamma emission but without detected radio radiation. Using the same data as for Equation (4) we can rewrite it in the following form

$$\log R_{\text{lum}1400} = (0.59 \pm 0.17) \log L_\gamma + 0.13 \pm 0.34. \quad (6)$$

Such potential radio emitters are listed in Table 3. We excluded the pulsar J1057–5226 because its value of \dot{E} does not satisfy the criterion $\dot{E} > 3 \times 10^{34} \text{ erg s}^{-1}$.

Table 3 contains values of pulsar periods, their gamma-ray luminosities and distances as listed in Abdo et al. (2013), expected radio luminosities calculated using Equation (6) and also expected flux densities at 1400 and 111 MHz. S_{1400} has been calculated by dividing $R_{\text{lum}1400}$ by d^2 . We have calculated expected values of S_{111} assuming the spectrum follows the power law

$$S_\nu = S_0 \nu^{-\alpha}. \quad (7)$$

Radio spectra of the pulsars from Table 3 are not known yet and we take the mean value of the spectral index $\alpha =$

Table 1 Considered Sample of Pulsars

	PSRJ	P (s)	$R_{lum1400}$ (mJy \times kpc ²)	\dot{E} (erg s ⁻¹)	B_{lc} (G)	L_{γ} 10 ³³ (erg s ⁻¹)
1	J0007+7303	0.316	*	4.5E+35	3.21E+03	94
2	J0030+0451	0.005	0.08	3.5E+33	1.83E+04	0.58
3	J0106+4855	0.083	0.07	2.9E+34	3.11E+03	21
4	J0205+6449	0.066	0.46	2.7E+37	1.19E+05	24
5	J0248+6021	0.217	54.8	2.1E+35	3.21E+03	25
6	J0340+4130	0.003	0.79	7.8E+33	4.04E+04	7.3
7	J0534+2200	0.033	56	4.5E+38	9.55E+05	619
8	J0631+1036	0.288	4.15	1.7E+35	2.18E+03	5.6
9	J0633+1746	0.237	*	3.2E+34	1.15E+03	31.7
10	J0659+1414	0.385	0.31	3.8E+34	7.66E+02	0.24
11	J0742–2822	0.167	60	1.4E+35	3.43E+03	9
12	J0835–4510	0.089	86.24	6.9E+36	4.45E+04	89.3
13	J0908–4913	0.107	10	4.9E+35	9.92E+03	35
14	J1016–5857	0.107	4.59	2.6E+36	2.26E+04	55
15	J1024–0719	0.005	2.23	5.3E+33	2.13E+04	0.06
16	J1028–5819	0.091	0.73	8.3E+35	1.51E+04	158
17	J1048–5832	0.124	54.66	2E+36	1.73E+04	176
18	J1057–5226	0.197	*	3E+34	1.33E+03	4.3
19	J1105–6107	0.063	4.18	2.5E+36	3.76E+04	150
20	J1112–6103	0.065	28.35	4.5E+36	4.95E+04	360
21	J1119–6127	0.408	56.45	2.3E+36	5.66E+03	600
22	J1124–5916	0.135	2	1.2E+37	3.85E+04	170
23	J1357–6429	0.166	4.23	3.1E+36	1.60E+04	25
24	J1410–6132	0.050	1095.12	1E+37	9.58E+04	800
25	J1418–6058	0.111	*	4.9E+36	3.04E+04	92
26	J1420–6048	0.068	28.43	1E+37	7.13E+04	640
27	J1509–5850	0.089	1.68	5.1E+35	1.22E+04	105
28	J1513–5908	0.151	18.2	1.7E+37	4.17E+04	70
29	J1531–5610	0.084	4.87	9.1E+35	1.71E+04	1
30	J1648–4611	0.165	11.59	2.1E+35	4.18E+03	160
31	J1658–5324	0.002	0.54	3E+34	1.08E+05	3
32	J1702–4128	0.182	17.34	3.4E+35	4.85E+03	80
33	J1709–4429	0.102	49.35	3.4E+36	2.72E+04	853
34	J1718–3825	0.075	15.83	1.3E+36	2.26E+04	138
35	J1730–3350	0.139	38.75	1.2E+36	1.20E+04	36
36	J1732–3131	0.197	*	1.5E+35	2.93E+03	8.6
37	J1741–2054	0.414	0.01	9.5E+33	3.55E+02	2.1
38	J1744–1134	0.004	0.48	5.2E+33	2.68E+04	0.68
39	J1747–2958	0.099	1.59	2.5E+36	2.42E+04	570
40	J1747–4036	0.002	46.01	1.2E+35	3.13E+05	40
41	J1801–2451	0.125	12.21	2.6E+36	1.95E+04	14
42	J1809–2332	0.147	*	4.3E+35	6.74E+03	164
43	J1833–1034	0.062	1.19	3.4E+37	1.42E+05	160
44	J1835–1106	0.166	21.97	1.8E+35	3.84E+03	6
45	J1907+0602	0.107	0.02	2.8E+36	2.38E+04	314
46	J1939+2134	0.002	161.7	1.1E+36	1.02E+06	14
47	J1952+3252	0.040	9	3.7E+36	7.38E+04	66
48	J2043+2740	0.096	*	5.6E+34	3.73E+03	3.8
49	J2124–3358	0.005	0.61	6.8E+33	2.52E+04	0.4
50	J2229+6114	0.052	2.25	2.2E+37	1.39E+05	19.4
51	J2240+5832	0.140	142.7	2.2E+35	5.08E+03	80

Table 2 Radio Pulsars with Expected Gamma Emission

	PSRJ	P (s)	$R_{\text{lum}1400}$ (mJy \times kpc ²)	L_{γ} 10^{33} (erg s ⁻¹)
1	J0117+5914	0.101	0.94	15.07 \pm 7.11
2	J0358+5413	0.156	23	58.39 \pm 45.54
3	J0535-6935	0.201	123.5	119.00 \pm 132.49
4	J0538+2817	0.143	3.21	25.35 \pm 13.22
5	J0540-6919	0.051	59.28	87.20 \pm 83.42
6	J0543+2329	0.246	21.9	57.19 \pm 44.13
7	J0614+2229	0.335	6.66	34.54 \pm 20.61
8	J0729-1448	0.252	5.07	30.77 \pm 17.39
9	J0820-3826	0.125	20.91	56.08 \pm 42.84
10	J0834-4159	0.121	5.77	32.50 \pm 18.84
11	J0855-4644	0.065	6.52	34.23 \pm 20.34
12	J0940-5428	0.088	0.1	5.83 \pm 3.80
13	J1015-5719	0.140	6.71	34.65 \pm 20.71
14	J1016-5819	0.088	2.08	21.10 \pm 10.37
15	J1019-5749	0.162	95.05	106.50 \pm 112.42
16	J1020-6026	0.140	1.5	18.37 \pm 8.77
17	J1052-5954	0.181	1.48	18.27 \pm 8.72
18 ^a	J1055-6028	0.100	11.44	43.44 \pm 29.07 (280)
19	J1138-6207	0.118	25.33	60.82 \pm 48.46
20 ^b	J1151-6108	0.102	0.3	9.29 \pm 4.88
21	J1156-5707	0.288	1.54	18.58 \pm 8.89
22	J1248-6344	0.198	13.74	46.94 \pm 32.70
23	J1301-6305	0.185	52.86	83.06 \pm 77.56
24	J1327-6400	0.281	61.12	88.33 \pm 85.06
25 ^b	J1341-6220	0.193	301.17	173.59 \pm 230.42
26	J1359-6038	0.128	190	142.82 \pm 173.31
27	J1400-6325	0.031	12.25	44.71 \pm 30.37
28	J1406-6121	0.213	19.34	54.26 \pm 40.74
29	J1412-6145	0.315	23.83	59.27 \pm 46.59
30	J1413-6141	0.286	44.59	77.29 \pm 69.60
31	J1437-5959	0.062	5.48	31.80 \pm 18.25
32	J1512-5759	0.129	280.71	168.49 \pm 220.64
33	J1514-5925	0.149	4.15	28.27 \pm 15.40
34	J1524-5625	0.078	9.48	40.11 \pm 25.78
35	J1538-5551	0.105	8.94	39.13 \pm 24.83
36	J1541-5535	0.296	5.88	32.76 \pm 19.07
37	J1548-5607	0.171	32.6	67.69 \pm 56.97
38	J1601-5335	0.288	2.8	23.93 \pm 12.22
39	J1611-5209	0.182	10.44	41.79 \pm 27.42
40	J1614-5048	0.232	63.65	89.86 \pm 87.27
41	J1632-4757	0.229	7.06	35.40 \pm 21.38
42	J1636-4440	0.207	59	87.02 \pm 83.17
43	J1637-4553	0.119	13.02	45.88 \pm 31.59
44	J1637-4642	0.154	15.1	48.86 \pm 34.74
45	J1638-4417	0.118	30.34	65.66 \pm 54.41
46	J1638-4608	0.278	6.89	35.04 \pm 21.06
47	J1643-4505	0.237	6.34	33.83 \pm 19.99
48	J1646-4346	0.232	38.28	72.45 \pm 63.14
49	J1702-4306	0.216	6.83	34.91 \pm 20.94
50	J1702-4310	0.241	13.44	46.50 \pm 32.24
51	J1705-3950	0.319	17.65	52.19 \pm 38.41
52	J1715-3903	0.278	6.4	33.96 \pm 20.10
53	J1721-3532	0.280	232.76	155.64 \pm 196.54
54	J1722-3712	0.236	19.68	54.66 \pm 41.20

Table 2 — *Continued.*

	PSRJ	P (s)	$R_{\text{lum}1400}$ (mJy \times kpc ²)	L_{γ} 10^{33} (erg s ⁻¹)
55	J1723–3659	0.203	18.38	53.10 \pm 39.43
56 ^c	J1739–3023	0.114	9.42	40.00 \pm 25.67 (16.2)
57	J1740+1000	0.154	13.92	47.20 \pm 32.97
58	J1743–3153	0.193	39.25	73.22 \pm 64.16
59	J1755–2534	0.234	3.29	25.62 \pm 13.41
60	J1757–2421	0.234	37.96	72.19 \pm 62.80
61	J1803–2137	0.134	269.1	165.51 \pm 214.97
62	J1809–1917	0.083	26.73	62.23 \pm 50.16
63	J1815–1738	0.198	5.98	33.00 \pm 19.27
64	J1825–1446	0.279	51.95	82.46 \pm 76.71
65	J1826–1334	0.101	27.37	62.85 \pm 50.93
66	J1828–1057	0.246	3.03	24.74 \pm 12.79
67 ^c	J1828–1101	0.072	65.98	91.24 \pm 89.28 (140)
68 ^c	J1831–0952	0.067	4.47	29.17 \pm 16.10
69	J1833–0827	0.085	72.9	95.18 \pm 95.10
70	J1835–0643	0.306	33.28	68.28 \pm 57.73
71	J1835–0944	0.145	7.3	35.91 \pm 21.84
72 ^c	J1837–0604	0.096	15.99	50.06 \pm 36.05 (370)
73	J1838–0453	0.381	14.73	48.34 \pm 34.19
74	J1838–0549	0.235	4.76	29.96 \pm 16.73
75	J1839–0321	0.239	16.43	50.63 \pm 36.68
76	J1841–0345	0.204	20	55.03 \pm 41.63
77	J1841–0425	0.186	50.34	81.36 \pm 75.19
78	J1841–0524	0.446	3.43	26.08 \pm 13.74
79 ^a	J1843–1113	0.002	0.16	7.12 \pm 4.20 (5.4)
80	J1845–0316	0.208	9	39.24 \pm 24.94
81	J1850–0026	0.167	79.69	98.84 \pm 100.60
82	J1853–0004	0.101	24.81	60.29 \pm 47.82
83	J1853+0056	0.276	3.1	24.98 \pm 12.96
84	J1856+0113	0.267	2.07	21.05 \pm 10.35
85	J1856+0245	0.081	23.17	58.57 \pm 45.76
86	J1857+0143	0.140	15.45	49.33 \pm 35.26
87	J1904+0800	0.263	43.16	76.23 \pm 68.17
88	J1907+0631	0.324	2.89	24.25 \pm 12.44
89	J1907+0918	0.226	19.59	54.55 \pm 41.08
90	J1909+0749	0.237	15.53	49.44 \pm 35.38
91	J1909+0912	0.223	20.27	55.35 \pm 41.99
92	J1913+0832	0.134	40.34	74.08 \pm 65.29
93 ^a	J1913+0904	0.163	2.02	20.84 \pm 10.21 (34)
94	J1913+1011	0.036	10.63	42.11 \pm 27.74
95	J1916+1225	0.227	3.96	27.71 \pm 14.97
96	J1917+1353	0.195	47.5	79.39 \pm 72.46
97	J1922+1733	0.236	33.24	68.25 \pm 57.69
98	J1925+1720	0.076	1.79	19.80 \pm 9.59
99	J1928+1746	0.069	5.26	31.25 \pm 17.79
100	J1930+1852	0.137	2.94	24.43 \pm 12.57
101	J1932+2220	0.144	142.57	126.46 \pm 144.93
102	J1934+2352	0.178	9.23	39.66 \pm 25.34
103	J1935+2025	0.080	11.15	42.97 \pm 28.60
104	J1938+2213	0.166	6.9	35.06 \pm 21.08
105	J1948+2551	0.197	47.08	79.09 \pm 72.05
106	J2004+3429	0.241	12.78	45.52 \pm 31.21
107	J2006+3102	0.164	9.82	40.72 \pm 26.37

References: ^a Hou X., Smith D.A., Guillemot L. et al., Hou et al. (2014); ^b Smith D.A., Guillemot L., Kerr M., Ng C., Barr E., Smith et al. (2017); ^c Laffon H., Smith D. A., Guillemot L., Laffon et al. (2015).

Table 3 Gamma-ray Pulsars with Expected Radio Emission

	PSRJ	P (s)	$R_{\text{lum}1400}$ (mJy \times kpc ²)	L_{γ}	d (kpc)	S_{1400} (mJy)	S_{111} (mJy)
1	J0007+7303	0.316	8.90	94	1.4	4.5	203.4
2	J0633+1746	0.237	5.35	31.7	0.25	85.6	3835.7
3	J1418–6058	0.111	8.81	92	1.6	3.4	154.2
4	J1732–3131	0.197	2.91	8.6	0.64	7.1	317.9
5	J1809–2332	0.147	11.55	164	1.7	4.0	179.0
6	J2043+2740	0.096	1.98	3.8	1.25	1.3	56.9

1.5 (Malov & Malofeev 2010) for all considered objects. In the frame of these suggestions we have

$$S_{111} = 44.8 \times S_{1400}. \quad (8)$$

These estimates show that pulsars from Table 3 can be registered in the radio range with high probability. The most promising candidates for gamma-ray pulsars in the Northern Hemisphere are J0007+7303 and J0633+1746.

5 CONCLUSIONS

The sample of pulsars detected as radio and/or gamma-ray emitters is presented. It is restricted to objects with losses of rotational energy $\dot{E} > 3 \times 10^{34} \text{ erg s}^{-1}$ and magnetic fields at the light cylinder $B_{\text{lc}} > 10^3 \text{ G}$.

Pulsars listed in the 2FGL catalog show a correlation between luminosities in the radio and gamma ranges. This correlation gives an opportunity to choose radio pulsars which can be detected as gamma-ray sources by *Fermi*/LAT. Using the same correlation, we propose to search for radio emission from several gamma-ray pulsars believed to be radio quiet up to now. It is worth noting that J0633+1746 has already been detected as a radio pulsar (see Malofeev & Malov 2002). This detection demonstrates that the proposed program of searching for new radio pulsars is quite reasonable.

We propose a program of observations using the Large Phased Antenna (LPA) at the Pushchino Radio Astronomy Observatory to search for radio emission from the objects in Table 3 at 111 MHz. The results of these observations will be published separately. This paper has been written on the basis of results presented to the All-Russian Astronomical Conference VAK-2017 (see the Preface Samus & Li (2018) in this issue).

Acknowledgements This work has been carried out with financial support of Basic Research Program of the Presidium of the Russian Academy of Sciences “Transitional and Explosive Processes in Astrophysics (P-41)” and Russian Foundation for Basic Research (grant 16–02–00954).

References

- Abdo, A. A., Ajello, M., Allafort, A., et al. 2013, *ApJS*, 208, 17
- Hou, X., Smith, D. A., Guillemot, L., et al. 2014, *A&A*, 570, A44
- Laffon, H., Smith, D. A., Guillemot, L., & for the Fermi-LAT Collaboration. 2015, arXiv:1502.03251
- Loginov, A. A., & Malov, I. F. 2014, *Astronomy Reports*, 58, 733
- Malofeev, V. M., & Malov, O. I. 2002, in *IAU Symposium*, 199, *The Universe at Low Radio Frequencies*, ed. A. Pramesh Rao, G. Swarup, & Gopal-Krishna, 393
- Malov, I. F., & Timirkeeva, M. A. 2014, *Astronomy Reports*, 58, 611
- Malov, I. F., & Timirkeeva, M. A. 2015, *Astronomy Reports*, 59, 865
- Malov, O. I., & Malofeev, V. M. 2010, *Astronomy Reports*, 54, 210
- Manchester, R. N., Hobbs, G. B., Teoh, A., & Hobbs, M. 2005, *AJ*, 129, 1993
- Pierbattista, M., Grenier, I. A., Harding, A. K., & Gonthier, P. L. 2012, *A&A*, 545, A42
- Samus, N. N., & Li, Y., *RAA (Research in Astronomy and Astrophysics)*, 2018, 18, 88
- Smith, D. A., Guillemot, L., Kerr, M., Ng, C., & Barr, E. 2017, arXiv:1706.03592
- Thompson D. J. 1996, *ASP Conference Series*, 105, 307